POSITRON RANGES OBTAINED FROM BIOMEDICALLY IMPORTANT POSITRON-EMITTING RADIONUCLIDES

Z. H. Cho, J. K. Chan, L. Ericksson, M. Singh, S. Graham, N. S. MacDonald, and Y. Yano

Laboratory of Nuclear Medicine and Radiation Biology, University of California, Los Angeles and Donner Laboratory and Lawrence Berkeley Laboratory, University of California, Berkeley

Positron ranges were obtained experimentally for several nuclides used in scintigraphic imaging. The nuclides examined were ^{11}C, ^{13}N, ^{15}O, ^{18}F, ^{68}Ga, and ^{82}Rb. The results are discussed with respect to the ultimate spatial resolution obtained in a scintigraphic image.

In recent times there has been renewed interest in scintigraphic imaging of positron emitters, particularly in connection with three-dimensional tomography using positron annihilation photon coincidence detection (*1–4*). This has prompted us to obtain more detailed information on positron ranges, penetration depths, and range distributions, which we believe are relevant to the final image resolution and ultimate design factors for positron cameras.

The terms "range" and "path length" (or sum of collision lengths) have been widely used in a somewhat ambiguous manner. According to well-known range–energy relations, the path length γ is given by the following (*5*):

$$\gamma(T) = \int_0^{T_0} \left[-\frac{1}{\rho} \left(\frac{dE}{dx} \right)_{coll} \right]^{-1} dt \qquad (1)$$

where $\frac{1}{\rho}\frac{dE}{dx}$ represents the stopping power of the medium and T is the kinetic energy of the electrons.

The path length has been misused as "range" on several occasions. The range, as defined in this paper, is strictly the penetration depth, which can be identified only by such statistical distribution quantities as FWHM and FW(1/10)M (i.e., 90% absorption thickness). The path length is interpreted as the integral of the reciprocal of the stopping power, i.e., the continuous slowing down approximation range. Since electrons and positrons follow a tortuous path in matter, due to elastic and inelastic scattering by atoms, the range derived from the continuous slowing down approximation appears much larger than the range defined in this paper. Also, since the "range" of the positron is so much smaller than the "path length" (*6–8*), and possibly smaller than the resolution of the camera itself (*9*), neither estimates from the range–energy table using the continuous slowing down approximation nor direct measurements using existing positron-imaging devices can correctly reveal the actual "range" or penetration depth, the factor that ultimately causes the image blurring.

In the present paper, the quantitative results of direct experimental determination of positron ranges are given for a number of clinically used positron-emitting radionuclides. Observation of the images obtained with existing imaging devices can only qualitatively describe the phenomenon (*10*). The purpose of the present paper is, therefore, to determine the "intrinsic" uncertainty in an image obtained with a positron-imaging device so that its clinical effect can be predicted.

EXPERIMENTAL ARRANGEMENT AND RESULTS

Figure 1 shows the experimental arrangement used for the determination of the absolute positron range distributions for six clinically useful radionuclides. The source, an aqueous solution of the radionuclide in a polystyrene tube (1.39 mm inner diameter), was moved in the y direction in a 38-mm-wide water tank placed between two carefully aligned well-shielded lead collimators of 3.17 mm diameter and 50.8 mm length.

Fast anode pulses from two NaI(Tl) + PM tube detectors were fed to the time-to-pulse-height converter through the time pick-off units (timing filter amplifier + constant fraction discriminator). The pulses within the time resolution of ±10 nsec were then selected by a single-channel analyzer and fed

---

Received April 7, 1975; revision accepted June 20, 1975.

For reprints contact: Z. H. Cho, Laboratory of Nuclear Medicine and Radiation Biology, University of California at Los Angeles, Los Angeles, Calif. 90024.

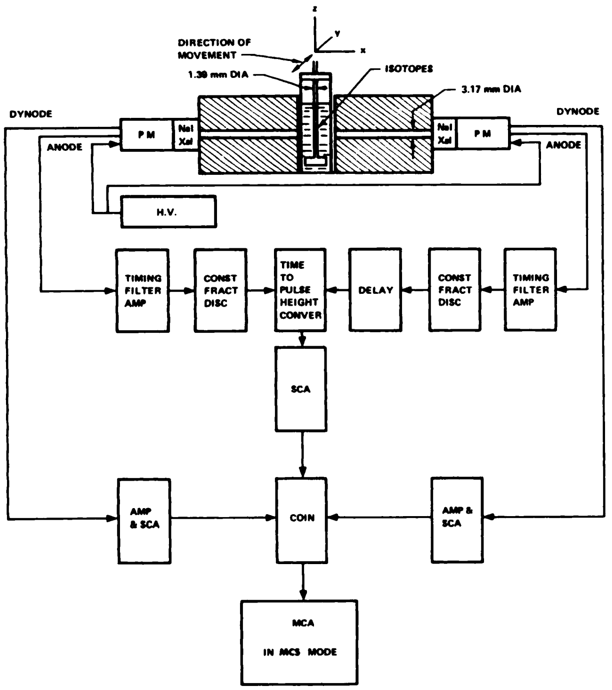

FIG. 1. Setup for positron range experiment.

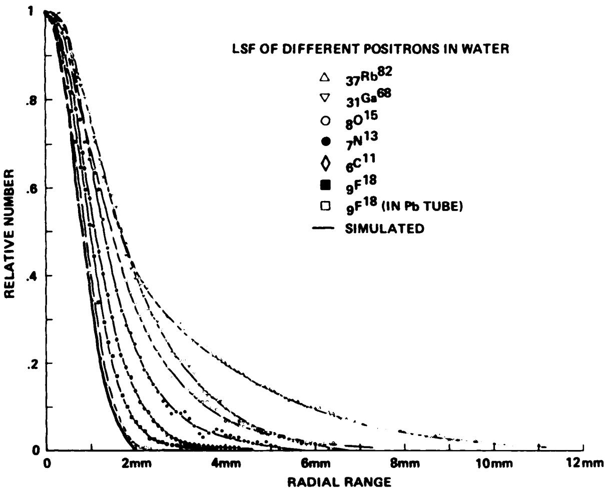

FIG. 2. Line spread functions of different positrons in water.

to the slow triple-coincidence unit. Coincident events fulfilling the present energy condition (the selected energy interval was 300–560 keV) were then fed to a multichannel analyzer operated in a multichannel scaling mode and synchronized with a motor that moved the source tube.

In Fig. 2, the experimentally observed range distributions are shown. The curve with open squares is the near-ideal case, namely zero positron range, obtained with a ^{18}F source sealed in a lead tube with 1.39 mm inner diameter and 1 mm thickness. This ideal experimental case (zero positron range) agrees very well with the computer-simulated results; the heavy line shown in the figure is the simulated result taking into account the line character of the tube. It also agrees with the 50% isosensitivity response at the center, which is 0.4 of the collimator radius. As expected, the broadening of the range distribution increases with the increase of the maximum and most probable energies of the emitted positrons.

Since the collimators' contribution to the range distribution is small for the high-energy positrons emitted from ^{15}O, ^{68}Ga, or ^{82}Sr*, the indicated FW(1/10)M is mainly due to the range of the positrons. One-half of the FW(1/10)M corresponds to the thickness of the material within which 90% of the particles are stopped, and it can be defined as the "effective range" R of the positrons. The ratio of R to the path length calculated by the continuous slowing down approximation (Eq. 1) is as low as one-third for ^{82}Sr and as high as one-half for ^{11}C.

It is uncertain why there is a substantial difference in FWHM between ^{15}O and ^{68}Ga and almost no difference between ^{68}Ga and ^{82}Rb (which has a much higher maximum as well as a higher most probable energy). The FW(1/10)M, however, is considerably different in either case.

Table 1 summarizes the maximum energies, most probable energies, half-lives, theoretically calculated path lengths, and FWHM and FW(1/10)M radial

---

* The notation ^{82}Rb or ^{82}Sr is used in this paper to represent an equilibrium mixture of ^{82}Rb and ^{82}Sr.

TABLE 1. POSITRON-EMITTING ISOTOPES

	^{18}F	^{11}C	^{13}N	^{15}O	^{68}Ga	^{82}Sr (^{82}Rb)
Maximum energy (MeV)	0.633	0.959	1.197	1.738	1.898	3.148
Most probable energy (MeV)	0.2025	0.326	0.432	0.696	0.783	1.385
Half-life (min)	109.7	20.3	10.0	2	68.3	1.3
Path length for electron of same maximum energy in water (cm)	0.239	0.498	0.535	0.822	0.908	1.561
Radial range in water (exp)* FWHM (cm)	0.102	0.111	0.142	0.149	0.168	0.169
Radial range in water (exp)* FW(1/10)M (cm)	0.18	0.219	0.278	0.357	0.395	0.58

* For line source of 0.1397 cm diameter with 0.3175-cm-diameter collimator.

ranges for the six most commonly used positron-emitting radionuclides.

CONCLUSION

The line spread functions produced by positron-emitting radionuclides are smaller than would be predicted solely on the basis of the conventional "range path length" concept. The main reasons are the tortuous path of a positron during collisions with atomic electrons, and the fact that the most probable energy is substantially lower than the indicated maximum energy.

Since actual line spread functions observed with most of the radionuclides were smaller than 3 mm FWHM, there will probably not be a significant loss in spatial resolution in actual scanners or cameras. It appears, however, that with high-energy positron emitters (e.g., ^{82}Sr) the line spread contribution due to a relatively large FW(1/10)M (11.6 mm) might affect images obtained with high-resolution positron cameras (*10–12*).

ACKNOWLEDGMENT

These studies were supported by United States Energy Research and Development Administration Contract AT (04-1) GEN-12 and the University of California.

REFERENCES

1. Brownell GL, Burnham CA, Wilensky S, et al: New developments in positron scintigraphy and the application of cyclotron produced positron emitters. In *Medical Radioisotope Scintigraphy*, Vienna, IAEA, 1968, pp 163–176

2. Phelps ME, Hoffman EJ, Mullani NA, et al: Application of annihilation coincidence detection to transaxial reconstruction tomography. *J Nucl Med* 16: 210–224, 1975

3. Llacer J, Cho ZH: Preliminary study of a Ge three-dimensional camera for positron emitting radioisotopes. *IEEE Trans Nucl Sci* NS-20: No 1, 282–293, 1973

4. Cho ZH, Eriksson L, Chan JK: A circular ring transverse axial positron camera. In *Reconstruction Tomography in Diagnostic Radiology and Nuclear Medicine*, Symposium held at San Juan, Puerto Rico, April 17–19, 1975

5. Berger MJ, Seltzer SM: Tables of energy losses and ranges of electrons and positrons. NASA, Report SP-3012, Washington, DC, 1964

6. Rohrlic F, Carlson BC: Positron–electron differences in energy loss and multiple scattering. *Phys Rev* 93: 38–44, 1954

7. Anger HO: Radioisotope cameras. In *Instrumentation in Nuclear Medicine*, vol 1, Hine GJ, ed, New York, Academic Press, 1967, pp 485–552

8. Brownell GL: Personal communication, 1975

9. Anger HO: Personal communication, 1975

10. Graham LS, MacDonald NS, Robinson GD, et al: Effect of positron energy on spatial resolution. *J Nucl Med* 14: 401–402, 1973

11. Yano Y, Budinger TF: On the use of an ^{82}Rb generator in conjunction with MGH positron camera for imaging the myocardium. Program and Abstracts, Society of Nuclear Medicine, Northern California Chapter Meeting, San Francisco, Oct 26, 1974

12. Phelps M, Hoffman E, Huang H, et al: Effect of positron range on spatial resolution. *J Nucl Med* 16: 649–652, 1975